

Characterization of Bamboo Nanocellulose Prepared by TEMPO-mediated Oxidation

Korawit Chitbanyong,^a Sasiprapa Pitiphatharaworachot,^a Sawitree Pisutpiched,^a Somwang Khantayanuwong,^a and Buapan Puangsin^{a,b,*}

The synthesis of TEMPO-oxidized bamboo cellulose nanofibrils (TOBCNs) was attempted using two locally available species in Thailand (*Dendrocalamus asper* and *D. membranaceus*). Bamboo powder was first delignified with NaClO₂. The obtained bamboo holocelluloses (BHs) were then oxidized *via* a TEMPO/NaBr/NaClO system in water at pH 10 for 2 h. The effects of NaClO addition level on the weight recovery ratio, carboxylate content, and nanofibrillation yield were studied. At a higher level of NaClO addition, the weight recovery ratio of TEMPO-oxidized bamboo holocelluloses (TOBHs) decreased from 90% to 70%, while the carboxylate content of TOBHs increased up to 0.8 mmol/g to 0.9 mmol/g for both species. Fourier transform infrared spectra indicated that C6-hydroxyl groups of cellulose were converted to negatively-charged carboxylate groups. After a gentle mechanical treatment with water, transparent liquid of TOBCNs were obtained after the removal of unwanted fraction, which gave a nanofibrillation yield of more than 90% at a NaClO addition level of 7.5 mmol/g to 15.0 mmol/g-BHs. Well individualized TOBCNs were successfully prepared and had a length of several microns and an average width of 5 nm to 7 nm under transmission electron microscopy. Thus, ultra-long TOBCNs are applicable for use as nano-reinforced polymer composites in non-food industries.

Keywords: Bamboo; Nanocellulose; 2,2,6,6-Tetramethylpiperidine-1-oxyl (TEMPO)

Contact information: a: Department of Forest Products, Faculty of Forestry, Kasetsart University, Bangkok 10900, Thailand; b: Center of Excellence for Bamboos, Kasetsart University, Bangkok 10900, Thailand; *Corresponding author: fforbpbpp@ku.ac.th

INTRODUCTION

Cellulose is a polymer that is found extensively on Earth and is a major component of the plant cell wall containing $\beta(1-4)$ linked anhydroglucose unit chain (Dufresne 2012). Plant fibers consist of highly crystalline cellulose nanofibrils with a width of a few nanometers (nm) and length of several micrometers (μm). These are packed in the form of microfibrils embedded in hemicelluloses and the lignin matrix of the cell wall (Wang *et al.* 2015). Cellulose materials have been gradually gaining global interest due to their potential properties (Isogai *et al.* 2011). Transparent and flexible films prepared from cellulose nanomaterials possess a high tensile strength and modulus of elasticity. High crystallinity results in an extremely low coefficient of thermal expansion when compared to that of petroleum-based polymers (Henriksson *et al.* 2008; Puangsin *et al.* 2013b). The densely-packed structure of each nanofiber gives it an excellent oxygen-barrier ability of a base polymer film that is comparable to the commercial polymers (Fukuzumi *et al.* 2009; Fujisawa *et al.* 2011).

Nanocellulose materials have also been used for the reinforcement of many polymers, which resulted in the improvement of mechanical properties (Torres *et al.* 2013; Cobut *et al.* 2014). It was demonstrated that cellulose from a natural resource could be used to replace synthetic materials in green electronic devices, as well as in biomedical, aerospace, and military applications (Huang *et al.* 2013; Nakagaito and Yano 2014; Morales-Narváez *et al.* 2015; Zhou *et al.* 2016).

However, as cellulose molecules are strongly bound by a hydrogen bond, nanofibrillation is needed prior to obtaining cellulose nanofibrils (Shinoda *et al.* 2012). Cellulose nanofibrils can only be prepared by mechanical disintegration (Abe *et al.* 2007; Abe and Yano 2010), but high demands of energy are required, and it is impossible to completely individualize cellulose nanofibrils from such methods. Therefore, chemical treatment becomes essential for the production of cellulose nanomaterials (Dufresne 2012; Puangsin *et al.* 2017). The 2,2,6,6-tetramethylpiperidine-1-oxyl (TEMPO)-mediated oxidation system is one such potential and efficient method to convert original plant cellulose to cellulose nanofibrils, with very little mechanical force needed to disrupt the structure of oxidized products and cellulose nanofibrils to be isolated (Isogai *et al.* 2011; Zhang *et al.* 2012). When oxidation occurs, the C6-hydroxyl groups on the surface of native cellulose are oxidized to carboxylate groups (Habibi *et al.* 2006; Shinoda *et al.* 2012), while the crystallinity and crystal width of the original sample are maintained (Okita *et al.* 2010). The TEMPO-oxidized products are mostly disintegrated to individual cellulose nanofibrils due to electrostatic repulsion of the carboxylate groups after nanofibrillation and removal of the undesired fraction (Fujisawa *et al.* 2011; Puangsin *et al.* 2013a). The obtained TEMPO-oxidized cellulose nanofibrils possess excellent tensile, gas-barrier, and thermal properties (Fukuzumi *et al.* 2010; Puangsin *et al.* 2013b; Kuramae *et al.* 2014).

Various sources of cellulose are used as a starting material for preparation of cellulose nanofibrils. Bamboo is one such interesting renewable cellulose resource because of its wide distribution, availability, rapid growth, easy handling, and desirable properties (Dransfield and Widjaja 1995; Alila *et al.* 2013). Additionally, it is used as a raw material for the production of naturally reinforcing cellulose fiber in the pulp and paper industry (He *et al.* 2008; Liu *et al.* 2010; Vena *et al.* 2013). Worldwide bamboo production is estimated at around 20 million tons annually (Amada *et al.* 1996; Choy and McKay 2005). In the last decade, several studies have shown that the bamboo resource, either solid bamboo or bamboo pulp, can be converted to micro- or nano-scale cellulose materials such as microfibrillated cellulose (Abe and Yano 2010; Zhang *et al.* 2010), cellulose nanofibrils (Chen *et al.* 2011a, 2011b; Puangsin *et al.* 2013a), or cellulose nanocrystals (Yu *et al.* 2012; Hu *et al.* 2014), as well as in the preparation of transparent nanocellulose films or cellulose-based nanocomposites (Chang *et al.* 2012; Puangsin *et al.* 2013b; Su *et al.* 2015).

In Thailand, even though there is a rich diversity of native bamboo species, research and development in the field of cellulose nanomaterial production is still lacking. In this study, bamboo holocelluloses (BHs) were prepared from two bamboo species, *D. asper* and *D. membranaceus*. The BHs were oxidized using the TEMPO-mediated oxidation system in water at a pH of 10 under various conditions. The chemical characteristics and structure of the obtained TEMPO-oxidized bamboo holocelluloses (TOBHs) were determined and subsequently subjected to nanofibrillation, followed by centrifugation to obtain the supernatant. The optical transmittance and morphology of TEMPO-oxidized bamboo cellulose nanofibrils (TOBCNs) were characterized.

EXPERIMENTAL

Materials

Culms of *Dendrocalamus asper* and *Dendrocalamus membranaceus* Munro, approximately 3-years-old, were obtained from the bamboo plantation located in Nakhon Ratchasima, Thailand. The chemicals TEMPO (Sigma-Aldrich, Darmstadt, Germany), sodium bromide (NaBr), sodium hydroxide (NaOH), acetic acid (CH₃COOH), sodium chlorite (NaClO₂), and sodium hypochlorite (NaClO) (Merck, Bangkok, Thailand) were of laboratory grade and used without further purification.

Chemical composition analysis

The cut bamboo samples with a diameter at breast height (DBH) of approximately 1.3 m above the ground, were powdered in a laboratory mill. The bamboo powder obtained was sieved through a 40-mesh aperture and retained on a 60-mesh aperture screen. The bamboo powder was then subjected to a chemical composition analysis. Alpha-cellulose, extractives, ash, and lignin content were determined according to TAPPI T203 om-09 (2009), TAPPI T204 cm-07 (2007), TAPPI T211 om-12 (2012), and TAPPI T222 om-11 (2011), respectively, and these were considered as constituting the main chemical composition of the two bamboo species.

Methods

Preparation of bamboo holocellulose

The bamboo powder that was sieved through a 40- to 60-mesh aperture was delignified with NaClO₂ and CH₃COOH at a pH between 4 and 5 and at 75 °C for a duration of 1 h, and this was repeated four times using fresh chemicals, according to the method proposed by Wise *et al.* (1946). The BHs were subsequently washed thoroughly with water by filtration using a glass filter (16 µm to 40 µm in pore size) and were kept in a wet state (solid content approximately 10%) at 4 °C. The morphology of bamboo holocellulose was observed using a tabletop scanning electron microscope (SEM, TM3030Plus; Hitachi, Tokyo, Japan).

Preparation of TEMPO-oxidized bamboo holocellulose

The never-dried BHs sample (1 g) was dispersed in 100 mL of water containing 0.016 g TEMPO and 0.1 g NaBr. The TEMPO-mediated oxidation in the TEMPO/NaBr/NaClO system was started by adding NaClO solution containing 3.0, 5.0, 7.5, 10.0, 12.5, and 15.0 mmol/g-BHs at room temperature, and a pH of 10 was maintained with the addition of 0.5 M NaOH using a pH meter for 2 h. The obtained TOBHs, the water-insoluble fraction, was then thoroughly washed with water by filtration using a glass filter (16 µm to 40 µm in pore size) and stored in wet state at 4 °C before further analyses. Weight recovery ratios of the TOBHs were calculated from dry weights before and after the oxidation. The carboxylate content of the TOBHs was determined according to TAPPI T237 cm-08 (2008). The morphology of the BHs dispersed in water was observed using an optical microscope (BX50; Olympus, Tokyo, Japan).

Preparation of TEMPO-oxidized bamboo cellulose nanofibrils

The never-dried TOBHs (50 mg) were suspended in 50 mL of water (solid content 0.1%, w/v). The suspension was sonicated for 8 min using an ultrasonic processor (VCX 750; Sonics & Materials, Newtown, CT, USA) with a 13-mm-diameter probe tip at 20 kHz

and 450 W output power. The obtained transparent liquid was an aqueous dispersion of TOBCNs. The unfibrillated or partly defibrillated fraction was removed by centrifugation using a refrigerated centrifuge (Suprema MX-307; Tomy Digital Biology, Tokyo, Japan) at 7500 rpm for 25 min. The nanofibrillation yield was calculated from the dry weights of TOBCN suspension before and after centrifugation. In addition, the morphology, length, and width of TOBCNs were observed and measured using a transmission electron microscope (TEM, HT7700; Hitachi, Tokyo, Japan) at 100 kV. The TOBCNs were dispersed in water at a solid content of 0.1% (w/v), and the light transmittance spectra were measured using a spectrophotometer (UV-1800; Shimadzu, Kyoto, Japan) at a wavelength range between 300 nm to 800 nm.

Fourier transform infrared (FTIR) spectroscopy

Dried BHs and TOBHs were analyzed using an attenuated total reflectance (ATR)-Fourier transform infrared (FTIR) spectrometer (ALPHA, Bruker BioSpin Corporation, Billerica, MA, USA). For each sample, the diamond crystal of the ATR accessory was allowed to contact directly with the sample for analysis. The FTIR spectra were collected between the wavenumber range of 4,000 cm^{-1} to 500 cm^{-1} , at a resolution of 4 cm^{-1} and an accumulation of 32 scans.

RESULTS AND DISCUSSION

Characterization of Bamboo Holocellulose

Bamboo culm samples were split into small pieces and then ground. The sieved powder of 40- to 60-mesh size was selected for chemical analysis. The chemical compositions of the two bamboo species are shown in Table 1. It was observed that these two bamboo species exhibited a slight difference in chemical composition, as shown in Table 1.

Table 1. Chemical Composition of *D. asper* and *D. membranaceus* Bamboo Species

Species	Holocellulose (%)	Alpha-cellulose (%)	Acid-insoluble Lignin (%)	Ash Content (%)
<i>D. asper</i>	71.8 ± 0.4 ^a	68.5 ± 0.1	28.7 ± 0.0	0.02 ± 0.0
<i>D. membranaceus</i>	74.3 ± 1.0	67.9 ± 0.3	27.6 ± 0.2	0.02 ± 0.0

^a The data are presented as mean ± standard deviation

The obtained bamboo powder possesses mainly rod-like shaped particles with other structures partly made by mechanically-individualized fiber fraction. These particles consist of fiber bundles originally bound to parenchymatous cells, as found in a natural bamboo culm. Fibrillated microfibers also appear on the surface of fiber or the fiber bundle cell wall during the process of bamboo powder extraction. After delignification, the color of bamboo powder changed from light brown to pale yellow and the surface of the holocellulose particle was cleaner than that of the powder as a result of the removal of some chemical composition (*i.e.*, hemicellulose, lignin, starch, and pectin) and the microfibrillated part of the cell wall. However, the morphologies of both *D. asper* and *D. membranaceus* holocellulose still held their original shape and size with a slight increase in the amount of chemically-individualized fiber fraction (Fig. 1).

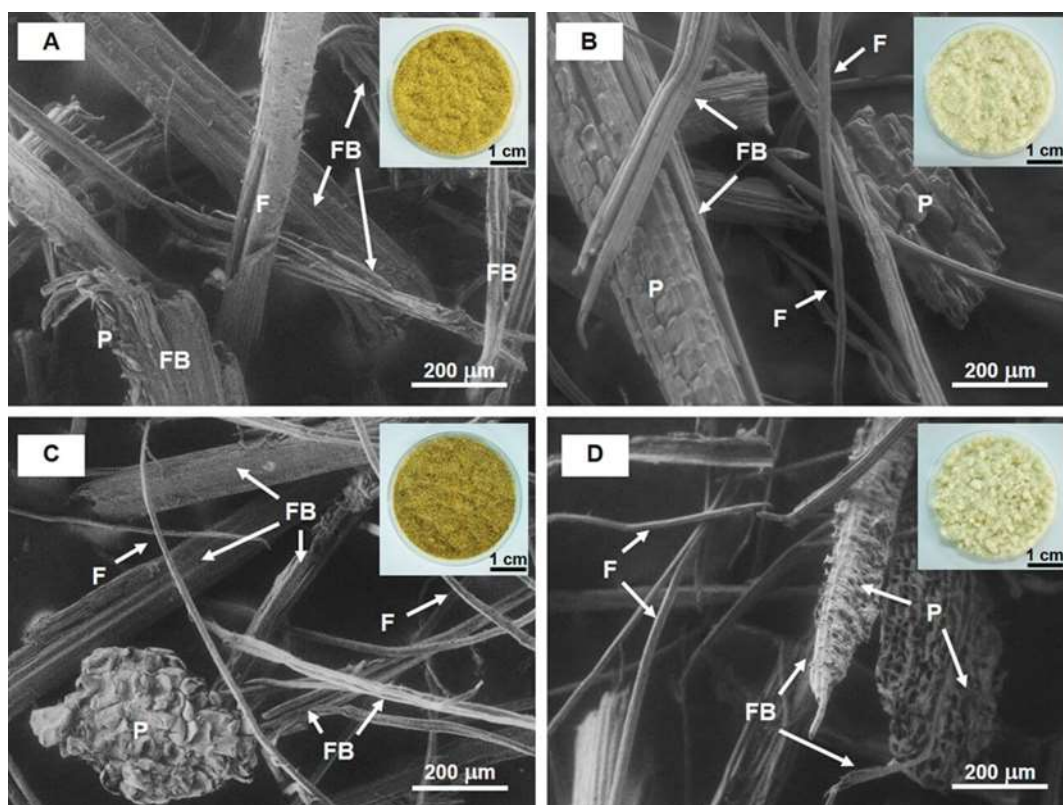


Fig. 1. SEM images together with inset photographs of *D. asper* (A) and *D. membranaceus* powder (C) and holocellulose (B and D) after delignification; magnified bamboo powder with holocellulose fiber, fiber bundle, and parenchymatous cell, are indicated by the acronyms F, FB, and P, respectively. The bamboo powder and holocellulose photographs are set to a scale of 1 cm.

TEMPO-mediated Oxidation of Bamboo Holocellulose

The BHs were oxidized with various NaClO addition levels (3.0 mmol/g to 15.0 mmol/g-BHs) in a TEMPO/NaBr/NaClO system at a pH of 10 and room temperature for 2 h and the resulting TOBHs were washed thoroughly with water. The relationship between the NaClO addition level and the weight recovery ratio or carboxylate content of TOBHs is shown in Fig. 2. At a higher NaClO addition level, the weight recovery ratio decreased from 89.5% to 69.1% for *D. asper* and from 88.4% to 73.8% for *D. membranaceus*. The oxidation behavior of the two bamboo species was almost similar. The TOBHs swelled to a balloon-like structure, became more gel-like, and changed in color from light yellow to white as the NaClO addition level was increased. In the range of 3.0 mmol/g to 5.0 mmol/g-BHs, the TOBH particle still retained some of the rod-like shape fiber bundles and an increased amount of single fiber due to the degradation of lignin and hemicellulose in the inter-cell matrices. From 7.5 mmol/g to 15.0 mmol/g-BHs, the rod-like shaped particle or fiber bundle was rarely observed and most of the fibers were largely swollen by TEMPO-mediated oxidation (Figs. 2 and 3).

The carboxylate content of TOBHs increased from 0.10 mmol/g to 0.92 mmol/g for *D. asper* and from 0.07 mmol/g to 0.84 mmol/g for *D. membranaceus*, which confirmed that the hydroxyl group on the cellulose surface was oxidized to a carboxylate group at higher levels of NaClO addition. However, at a NaClO addition level of 3.0 mmol/g-BHs,

the holocellulose content in the two bamboo samples was similar (0.09 mmol/g and 0.07 mmol/g in *D. asper* and *D. membranaceus*, respectively), due to the reaction of NaClO and holocellulose characteristics. At the beginning of oxidation, NaClO was added to the system as an oxidant. Apart from the catalysis of TEMPO and NaBr, NaClO also simultaneously reacted with hemicellulose and lignin to degrade the water-soluble forms, which were removed during the washing process (Isogai *et al.* 2011; Ma *et al.* 2012). Therefore, a loss in weight recovery ratio occurred, while the carboxylate content of TOBHs increased. As the alpha-cellulose content of *D. asper* was 68.5% and that for *D. membranaceus* was 67.9%, the BHs contained rather high amounts of hemicellulose and lignin.

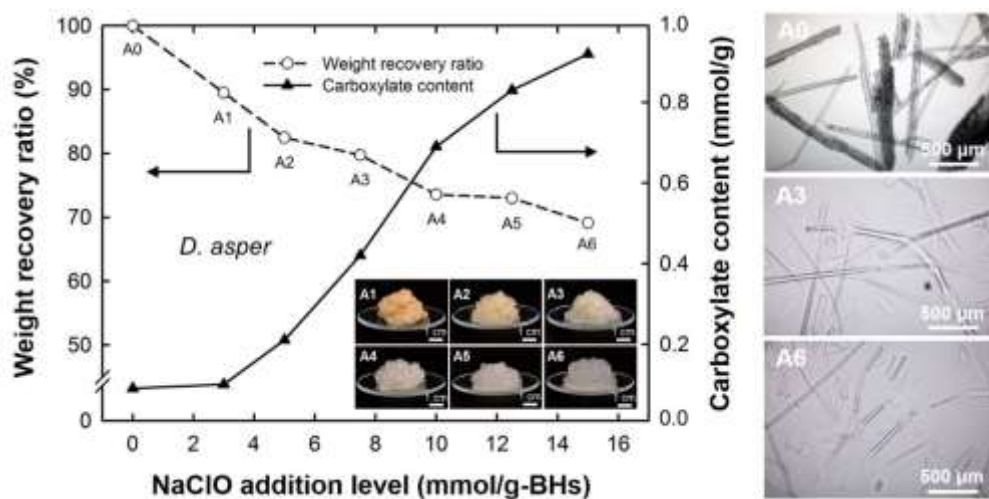


Fig. 2. Relationship between the NaClO addition level and the weight recovery ratio or carboxylate content of *D. asper* with inset photographs of TEMPO-oxidized bamboo holocelluloses (A1-A6). Optical microphotographs are of *D. asper* holocellulose (A0), and TOBH products (A3, and A6).

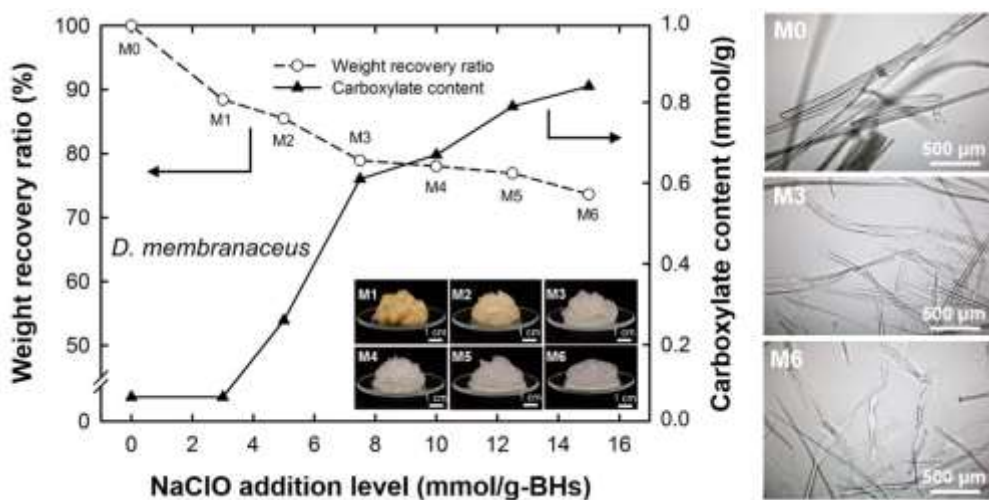


Fig. 3. Relationship between the NaClO addition level and the weight recovery ratio or carboxylate content of *D. membranaceus* with inset photographs of TEMPO-oxidized bamboo holocelluloses (M1-M6). Optical microphotographs are of *D. membranaceus* holocellulose (M0), and TOBH products (M3 and M6).

At the maximum NaClO addition level, the carboxylate content of BHs still remained less than 1.0 mmol/g, as the high level of residual lignin and hemicellulose present in the BHs caused a lower efficiency in the formation of carboxylate groups after oxidation, because it consumed chemicals during TEMPO-mediated oxidation (Okita *et al.* 2009; Kuramae *et al.* 2014).

The FTIR spectra of BHs and TOBHs of *D. asper* and *D. membranaceus* are illustrated in Fig. 4.

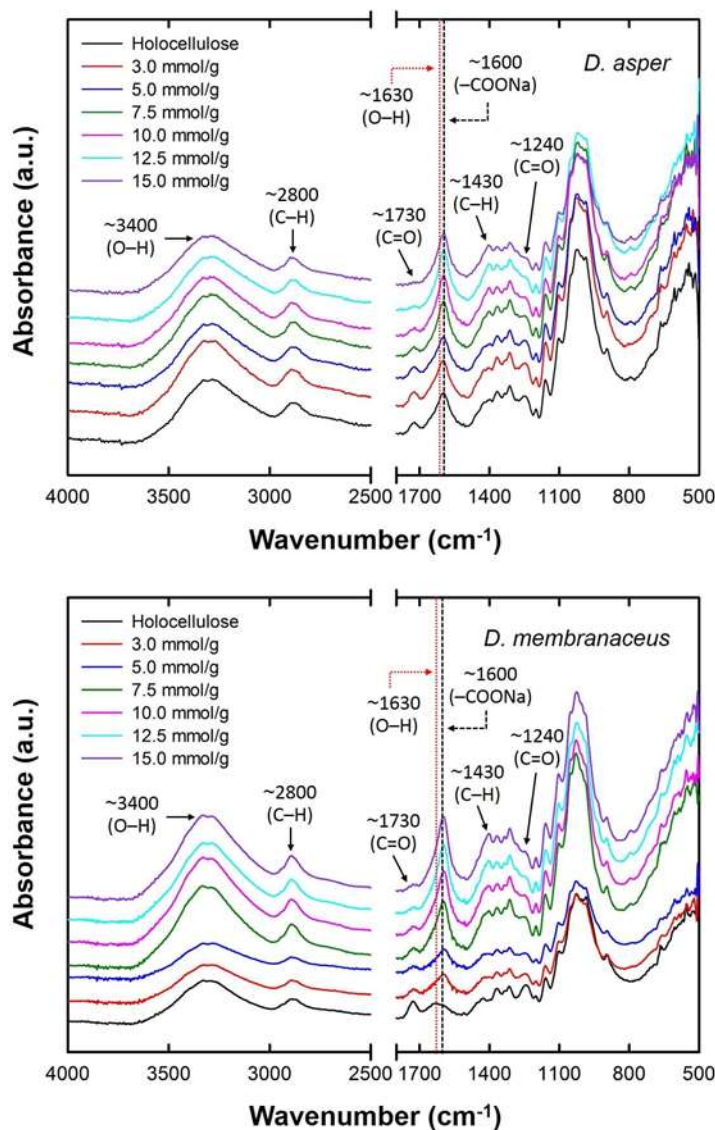


Fig. 4. FTIR spectra of BHs and TOBH products of *D. asper* and *D. membranaceus*

The broad peaks at approximately 3,400 cm^{-1} and approximately 2,800 cm^{-1} were due to the O–H stretching of the hydroxyl or carboxyl groups and C–H stretching of CH_2 , respectively (Alemdar and Sain 2008; Yu *et al.* 2012; Hu *et al.* 2014). The peaks at approximately 1,730 cm^{-1} and 1,240 cm^{-1} were associated with C=O stretching and vibration, indicating the presence of hemicellulose, phenolic acids, pectin, and xylan (Chen *et al.* 2011, 2015; Hu *et al.* 2014) and the C–O stretching of the aryl group in lignin (Jonoobi *et al.* 2009; Kargarzadeh *et al.* 2012; Karimi *et al.* 2014). Thus, the disappearance

of these peaks with the increasing levels of the NaClO addition in both BHs species indicated that hemicellulose and lignin were removed during oxidation. For BHs, the peak at approximately 1630 cm^{-1} represented the water absorption of hydrophilic O–H radicals in cellulose (Alemdar and Sain 2008; Yu *et al.* 2012; Hu *et al.* 2014; Chen *et al.* 2015). As the BHs were treated with NaClO in the TEMPO-mediated oxidation system, the peak slightly shifted from approximately $1,630\text{ cm}^{-1}$ to approximately $1,600\text{ cm}^{-1}$, which reconfirmed the observation that the carboxylate groups were introduced to the cellulose structure (Cobut *et al.* 2014). The band centered at approximately $1,430\text{ cm}^{-1}$ can be attributed to the characteristics of C–H stretching (He *et al.* 2008; Chen *et al.* 2011) or CH_2 symmetric bending of the degraded products or C=C stretching in lignin or hemicellulose structure (Le Troedec *et al.* 2008; Karimi *et al.* 2014).

TEMPO-oxidized Bamboo Cellulose Nanofibrils

After oxidation in the TEMPO/NaBr/NaClO-mediated system, TOBH products were mechanically disintegrated in water under the same conditions described above. Figure 5 shows the snapshots and optical UV-visible transmittance spectra of 1% (w/v) TOBCN dispersions.

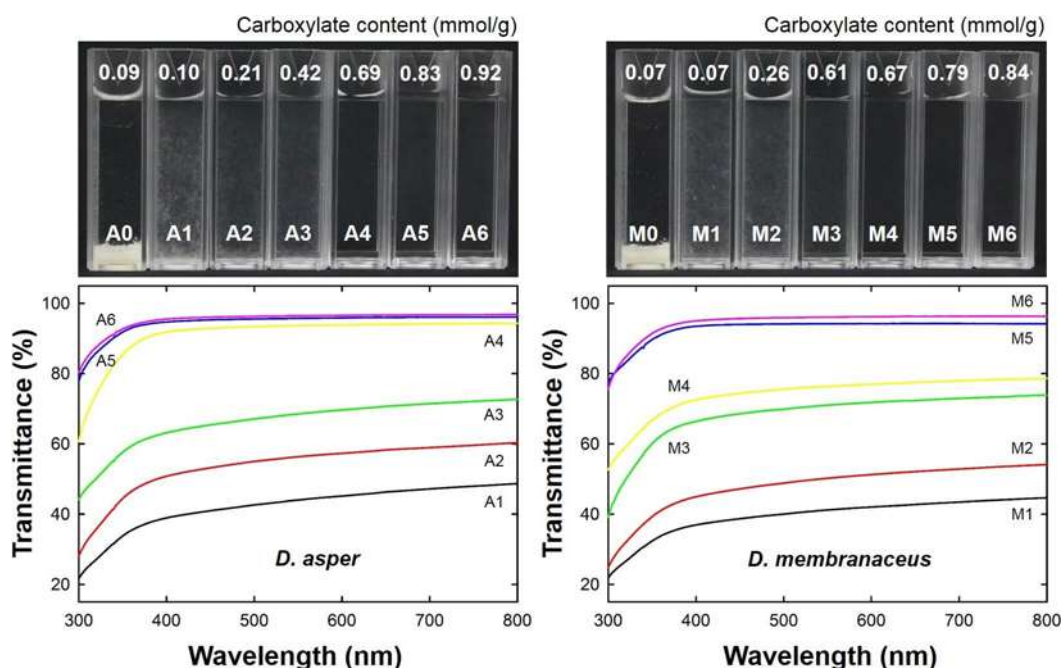


Fig. 5. Photographs and light transmittance spectra and of 0.1% TOBH dispersions without centrifugation

As the NaClO addition level and carboxylate content of TOBHs increased, the light transparency of TOBCN dispersions also increased. A transparent liquid of TOBCN dispersion was obtained without centrifugation when the carboxylate content reached 0.69 mmol/g and 0.67 mmol/g, at the NaClO addition level of 10.0 mmol/g-BHs, for *D. asper* and *D. membranaceus*, respectively. After the removal of the unfibrillated or partially fibrillated fraction by centrifugation of TOBCN dispersions, the nanofibrillation yield was calculated from the ratio of oven-dried before and after centrifugation weight. Figure 6 exhibits the relationship between the nanofibrillation yield and the NaClO addition level.

For *D. asper*, the nanofibrillation yield increased from 36.7% to 99.3% and from 24.3% to 97.1% for the *D. membranaceus*. Note that at 7.5 mmol/g NaClO addition, the nanofibrillation yield increased up to approximately 90% for both species.

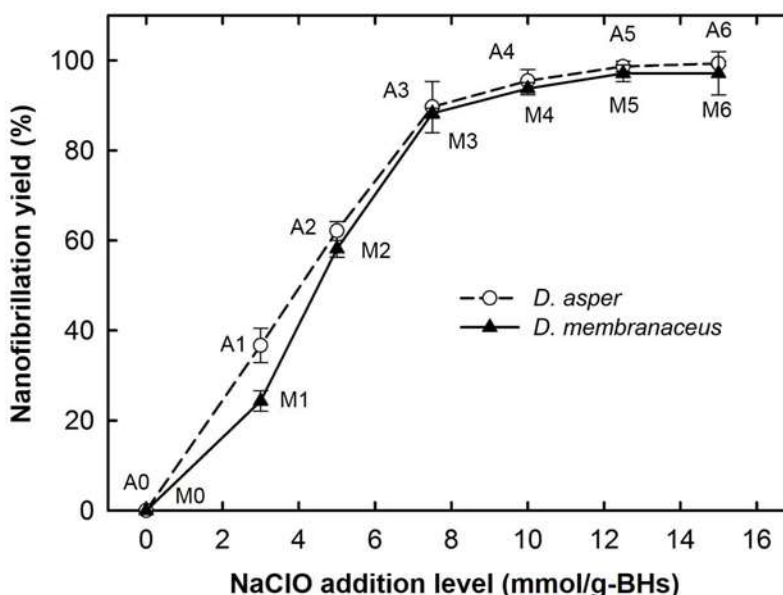


Fig. 6. Relationship between NaClO addition level and nanofibrillation yield of TOBHs for *D. asper* and *D. membranaceus*

At higher levels of NaClO addition, with an increasing carboxyl content and as the C6-carboxylate groups were introduced sufficiently to the surface of TOBCNs, electrostatic repulsion occurred due to negative charges, and mostly individualized TOBCNs were obtained. Meanwhile, TOBCNs were defibrillated to a size of a few nanometers, which did not scatter the visible light and the dispersion became transparent (Rodionova *et al.* 2013).

Figures 7 and 8 shows the TEM images and width distribution of TOBCNs prepared from mechanically disintegrated TOBHs. After being stained with uranyl acetate on copper grids, the widths of TOBCNs were measured using TEM. The resulting TOBCNs were well individualized and exhibited almost a similar morphology. However, at a length of > 1 μm , TOBCNs formed aggregates and were difficult to observe individually. At the lowest level of oxidation (3.0 mmol/g-BHs), the width distribution of the *D. asper* TOBCNs ranged widely from 3 nm to 15 nm, and when the oxidation level was further increased, the higher width distribution became slightly narrower and ranged between 3 nm to 11 nm. For *D. membranaceus*, the width distribution also ranged widely from 3 nm to 14 nm at a NaClO addition level of 3.0 mmol/g-BHs and became slightly narrower with a range of 3 nm to 10 nm. Both *D. asper* and *D. membranaceus* TOBCNs had an average width of 5 nm to 7 nm, which is comparable to bamboo pulp cellulose nanofibrils (2 nm to 6 nm) from the same process (Puangsin *et al.* 2013b) and those from solid bamboo (2 nm to 5 nm) (Chen *et al.* 2015). However, the width of TOBCNs was still smaller than that of bamboo nanocrystalline cellulose (< 20 nm) (Yu *et al.* 2012) and those obtained from a chemi-ultrasonic process (Chen *et al.* 2011b). It should be noted that under TEM observation, the width of the nanocellulose could be larger, as it could attach its longer side to the TEM grids (Saito *et al.* 2012).

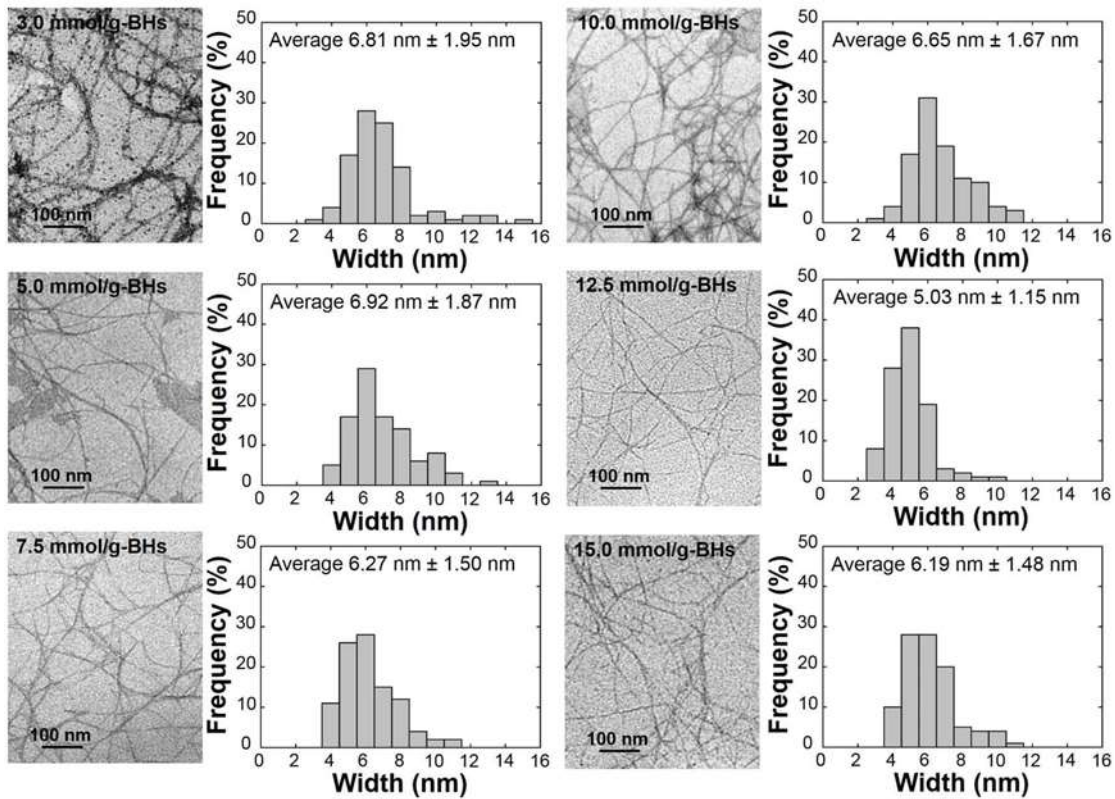


Fig. 7. TEM images and width distribution of TOBCNs for *D. asper*

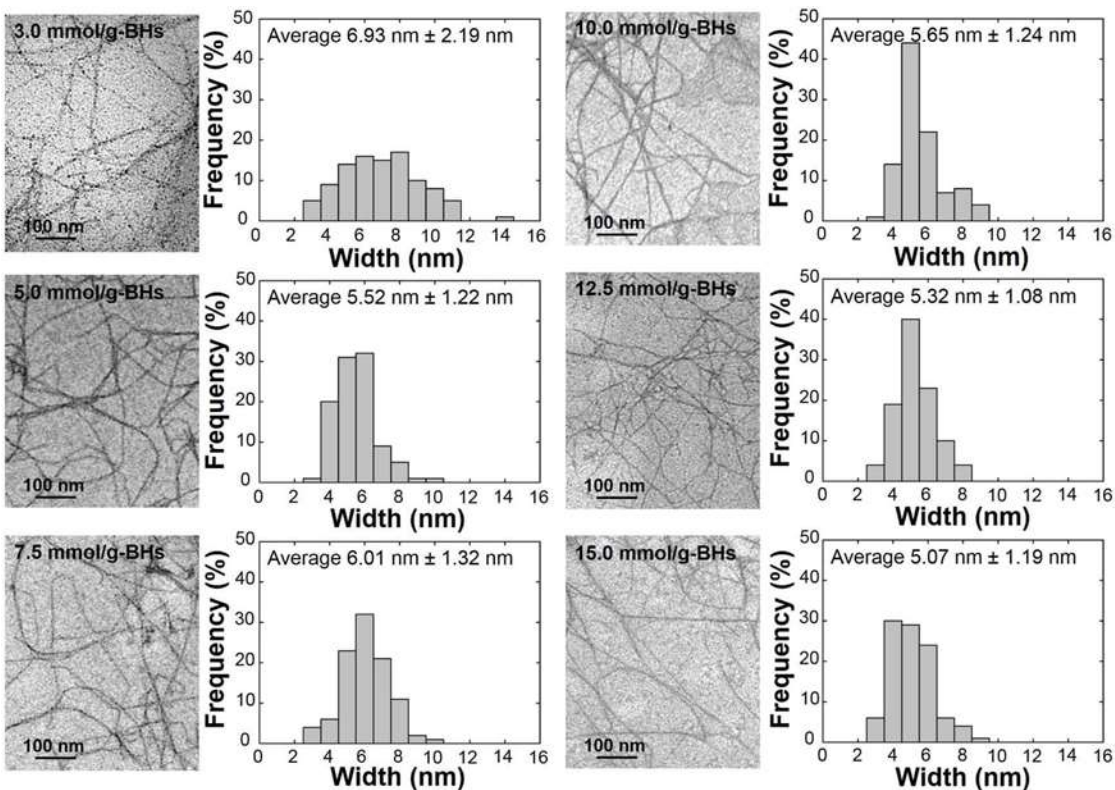


Fig. 8. TEM images and width distribution of TOBCNs for *D. membranaceus*

CONCLUSIONS

1. TEMPO-oxidized bamboo cellulose nanofibrils were successfully prepared from *Dendrocalamus asper* and *D. membranaceus* holocellulose by TEMPO/NaBr/NaClO oxidation in water at a pH of 10 and with a gentle mechanical treatment.
2. The formation of C6-carboxylate took place on the surfaces of cellulose microfibrils after TEMPO-mediated oxidation, which contributed to good dispersibility as a result of electrostatic repulsion between the negatively charged TOBCNs.
3. The TEMPO-oxidized BHs at NaClO addition levels between 10.0 mmol/g to 15.0 mmol/g-BHs were converted to a transparent dispersion without centrifugation, with a nanofibrillation yield of more than 90% from 7.5 mmol/g to 15.0 mmol/g-BHs.
4. The TEM results revealed that individualized TOBCNs were several microns long with an average approximate width of 5 nm to 7 nm.

ACKNOWLEDGMENTS

This research was supported by the Center of Excellence for Bamboos, Kasetsart University, Thailand.

REFERENCES CITED

- Abe, K., Iwamoto, S., and Yano, H. (2007). "Obtaining cellulose nanofibers with a uniform width of 15 nm from wood," *Biomacromolecules* 8(10), 3276-3278. DOI: 10.1021/bm700624p
- Abe, K., and Yano, H. (2010). "Comparison of the characteristics of cellulose microfibril aggregates isolated from fiber and parenchyma cells of Moso bamboo (*Phyllostachys pubescens*)," *Cellulose* 17(2), 271-277. DOI: 10.1007/s10570-009-9382-1
- Alemdar, A., and Sain, M. (2008). "Isolation and characterization of nanofibers from agricultural residues – Wheat straw and soy hulls," *Bioresource Technol.* 99(6), 1664-1671. DOI: 10.1016/j.biortech.2007.04.029
- Alila, S., Besbes, I., Vilar, M. R., Mutjé, P., and Boufi, S. (2013). "Non-woody plant as raw materials for production of microfibrillated cellulose (MFC): A comparative study," *Ind. Crop. Prod.* 41, 250-259. DOI: 10.1016/j.indcrop.2012.04.028
- Amada, S., Munekata, T., Nagase, Y., Ichikawa, Y., Kirikai, A., and Zhifei, Y. (1996). "The mechanical structures of bamboos in viewpoint of functionally gradient and composite materials," *J. Compos. Mater.* 30(7), 800-819. DOI: 10.1177/002199839603000703
- Chang, F., Lee, S. H., Toba, K., Nagatani, A., and Endo, T. (2012). "Bamboo nanofiber preparation by HCW and grinding treatment and its application for nanocomposite," *Wood Sci. Technol.* 46(1-3), 393-403. DOI: 10.1007/s00226-011-0416-0
- Chen, W., Li, Q., Cao, J., Liu, Y., Li, J., Zhang, J., Luo, S., and Yu, H. (2015). "Revealing the structure of cellulose nanofiber bundles obtained by mechanical

- nanofibrillation via TEM observation,” *Carbohydr. Polym.* 117, 950-956. DOI: 10.1016/j.carbpol.2014.10.024
- Chen, W., Yu, H., and Liu, Y. (2011a). “Preparation of millimeter-long cellulose I nanofiber with diameter of 30-80 nm from bamboo powder,” *Carbohydr. Polym.* 86(2), 453-461. DOI: 10.1016/j.carbpol.2011.04.061
- Chen, W., Yu, H., Liu, Y., Hai, Y., Zhang, M., and Chen, P. (2011b). “Isolation and characterization of cellulose nanofibers from four plant cellulose fibers using chemical-ultrasonic process,” *Cellulose* 18(2), 433-442. DOI: 10.1007/s10570-011-9497-z
- Choy, K. K. H., and McKay, J. P. (2005). “Production of activated carbon from bamboo scaffolding waste—process design, evaluation and sensitivity analysis,” *Chem. Eng. J.* 109(1-3), 147-165. DOI: 10.1016/j.cej.2005.02.030
- Cobut, A., Sehaqui, H., and Berglund, L. A. (2014). “Cellulose nanocomposites by melt compounding of TEMPO-treated wood fibers in thermoplastic starch matrix,” *BioResources* 9(2), 3276-3289. DOI: 10.15376/biores.9.2.3276-3289
- Dufresne, A. (2012). *Nanocellulose*, Walter de Gruyter, Berlin, Germany.
- Fujisawa, S., Okita, Y., Fukuzumi, H., Saito, T., and Isogai, A. (2011). “Preparation and characterization of TEMPO oxidized cellulose nanofibril films with free carboxyl groups,” *Carbohydr. Polym.* 84(1), 579-583. DOI: 10.1016/j.carbpol.2010.12.029
- Fukuzumi, H., Saito, T., Iwata, I., Kumamoto, Y., and Isogai, A. (2009). “Transparent and high gas barrier films from cellulose nanofibers prepared by TEMPO-mediated oxidation,” *Biomacromolecules* 10(1), 162-165. DOI: 10.1021/bm801065u
- Fukuzumi, H., Saito, T., Okita, Y., and Isogai, A. (2010). “Thermal stabilization of TEMPO-oxidized cellulose,” *Polym. Degrad. Stabil.* 95(9), 1502-1508. DOI: 10.1016/j.polymdegradstab.2010.06.015
- Habibi, Y., Chanzy, H., and Vignon, M. R. (2006). “TEMPO-mediated surface oxidation of cellulose whiskers,” *Cellulose* 13(6), 679-687. DOI: 10.1007/s10570-006-9075-y
- He, J., Cui, S., and Wang, S. (2008). “Preparation and crystalline analysis of high grade bamboo dissolving pulp for cellulose acetate,” *J. Appl. Polym. Sci.* 107(2), 1029-1038. DOI: 10.1002/app.27061
- Henriksson, M., Burglund, L. A., Isaksson, P., Linström, T., and Nishino, T. (2008). “Cellulose nanopaper structure of high toughness,” *Biomacromolecules* 9(6), 1579-1585. DOI: 10.1021/bm800038n
- Hu, Y., Tang, L., Lu, Q., Wang, S., Chen, X., and Huang, B. (2014). “Preparation of cellulose and carboxylated cellulose nanocrystals from borer powder of bamboo,” *Cellulose* 21(3), 1611-1618. DOI: 10.1007/s10570-014-0236-0
- Huang, J., Zhu, H., Chen, Y., Preston, C., Rohbach, K., Cumings, J., and Hu, L. (2013). “Highly transparent and flexible nanopaper transistors,” *ACS Nano* 7(3), 2106-2113. DOI: 10.1021/nn304407r

- Isogai, A., Saito, T., and Fukuzumi, H. (2011). "TEMPO-oxidized nanofibers," *Nanoscale* 3(1), 71-85. DOI: 10.1039/C0NR00583E
- Jonoobi, M., Harun, J., Shakeri, A., Misra, M., and Oksman, K. (2009). "Chemical composition, crystallinity, and thermal degradation of bleached and unbleached kenaf bast (*Hibiscus cannabinus*) pulp and nanofibers," *BioResources* 4(2), 626-639. DOI: 10.15376/biores.4.2.626-639
- Kargarzadeh, H., Ahmad, I., Abdullah, I., Dufresne, A., Zainudin, S. Y., and Sheltami, R. M. (2012). "Effects of hydrolysis conditions on the morphology, crystallinity, and thermal stability of cellulose nanocrystals extracted from kenaf bast fibers," *Cellulose* 19(3), 855-866. DOI: 10.1007/s10570-012-9684-6
- Karimi, S., Tahir, P. M., Karimi, A., Dufresne, A., and Abdulkhani, A. (2014). "Kenaf bast cellulosic fibers hierarchy: A comprehensive approach from micro to nano," *Carbohydr. Polym.* 101, 878-885. DOI: 10.1016/j.carbpol.2013.09.106
- Kuramae, R., Saito, T., and Isogai, A. (2014). "TEMPO-oxidized cellulose nanofibrils prepared from various plant holocelluloses," *React. Funct. Polym.* 85, 126-133. DOI: 10.1016/j.reactfunctpolym.2014.06.011
- Liu, D. G., Zhong, T. H., Chang, P. R., Li, K. F., and Wu, Q. L. (2010). "Starch composites reinforced by bamboo cellulosic crystals," *Bioresource Technol.* 101(7), 2529-2536. DOI: 10.1016/j.biortech.2009.11.058
- Ma, P., Fu, S., Zhai, H., Law, K., and Daneault, C. (2012). "Influence of TEMPO-mediated oxidation on the lignin of thermomechanical pulp," *Bioresource Technol.* 118, 607-610. DOI: 10.1016/j.biortech.2012.05.037
- Morales-Narváez, E., Golmohammadi, H., Nagdi, T., Yousefi, H., Kostiv, U., Horák, D., Pourreza, N., and Merkoçi, A. (2015). "Nanopaper as an optical sensing platform," *ACS Nano* 9(7), 7296-7305. DOI: 10.1021/acsnano.5b03097
- Nakagaito, A. N., and Yano, H. (2014). "Cellulose-nanofiber-based materials," in: *Cellulose Based Composites: New Green Nanomaterials*, J. P. Hinestroza and A. N. Netravali (eds.), Wiley-VCH Verlag, Weinheim, Germany, pp. 3-25.
- Okita, Y., Saito, T., and Isogai, A. (2009). "TEMPO-mediated oxidation of softwood thermomechanical pulp," *Holzforchung* 63(5), 529-535. DOI: 10.1515/HF.2009.096
- Okita, Y., Saito, T., and Isogai, A. (2010). "Entire surface oxidation of various cellulose microfibrils by TEMPO-mediated oxidation," *Biomacromolecules* 11(6), 1696-1700. DOI: 10.1021/bm100214b
- Puangsin, B., Fujisawa, S., Kuramae, R., Saito, T., and Isogai, A. (2013a). "TEMPO-mediated oxidation of hemp bast holocellulose to prepare cellulose nanofibrils dispersed in water," *J. Polym. Environ.* 21(2), 555-563. DOI: 10.1007/s10924-012-0548-9
- Puangsin, B., Soeta, H., Saito, T., and Isogai, A. (2017). "Characterization of cellulose nanofibrils prepared by direct TEMPO-mediated oxidation of hemp bast," *Cellulose* 24(9), 3767-3775. DOI: 10.1007/s10570-017-1390-y
- Puangsin, B., Yang, Q., Saito, T., and Isogai, A. (2013b). "Comparative characterization of TEMPO-oxidized cellulose nanofibril films prepared from non-wood resources," *Int. J. Biol. Macromol.* 59, 208-213. DOI: 10.1016/j.ijbiomac.2013.04.016

- Rodionova, G., Saito, T., Lenes, M., Eriksen, Ø., Gregersen, Ø., Kuramae, R., and Isogai, A. (2013). "TEMPO-mediated oxidation of Norway spruce and eucalyptus pulps: Preparation and characterization of nanofibers and nanofiber dispersions," *J. Polym. Environ.* 21(1), 207-214. DOI: 10.1007/s10924-012-0483-9
- Saito, T., Kuramae, R., Wohler, J., Berglund, L. A., and Isogai, A. (2012). "An ultralong nanofibrillar biomaterial: The strength of single cellulose nanofibrils revealed via sonication-induced fragmentation," *Biomacromolecules* 14(1), 248-253. DOI: 10.1021/bm301674e
- Shinoda, R., Saito, T., Okita, Y., and Isogai, A. (2012). "Relationship between length and degree of polymerization of TEMPO-oxidized cellulose nanofibrils," *Biomacromolecules* 13(3), 842-849. DOI: 10.1021/bm2017542
- Su, Y., Burger, C., Ma, H., Chu, B., and Hsiao, B. S. (2015). "Morphological and property investigations of carboxylated cellulose nanofibers extracted from different biological species," *Cellulose* 22(5), 3127-3135. DOI: 10.1007/s10570-015-0698-8
- TAPPI T203 om-09 (2009). "Alpha-, beta-, gamma-cellulose in pulp," TAPPI Press, Atlanta, GA.
- TAPPI T204 om-07 (2007). "Solvent extractives of wood and pulp," TAPPI Press, Atlanta, GA.
- TAPPI T211 om-12 (2012). "Ash in wood, pulp, paper and paperboard: Combustion at 525 °C," TAPPI Press, Atlanta, GA.
- TAPPI T222 om-02 (2002). "Acid-insoluble lignin in wood and pulp," TAPPI Press, Atlanta, GA.
- TAPPI T237 cm-08 (2008). "Carboxyl content of pulp," TAPPI Press, Atlanta, GA.
- Torres, F. G., Troncoso, O. P., Torres, C., and Grande, C. J. (2013). "Cellulose based blends, composites and nanocomposites," in: *Advances in Natural Polymers: Composites and Nanocomposites*, S. Thomas, P. M. Visakh, and A. P. Mathew (eds.), Springer-Verlag, Berlin, Germany, pp. 21-54.
- Vena, P. F., Brienzo, M., García-Aparicio, M. P., Görgens, J. F., and Rypstra, T. (2013). "Hemicelluloses extraction from giant bamboo (*Bambusa balcooa* Roxburgh) prior to kraft or soda-AQ pulping and its effect on pulp physical properties," *Holzforschung* 67(8), 863-870. DOI: 10.1515/hf-2012-0197
- Wang, H., Zhang, X., Jiang, Z., Li, W., and Yu, Y. (2015). "A comparison study of nanocellulose fibrils from fibers and parenchymal cells in bamboo (*Phyllostachys pubescens*)," *Ind. Crop. Prod.* 71, 80-88. DOI: 10.1016/j.indcrop.2015.03.086
- Wise, L. E., Murphy, M., and d'Addieco, A. A. (1946). "Chlorite holocellulose, its fractionation and bearing on summative wood analysis and on studies on the hemicelluloses," *Paper Trade Journal* 122(2), 35-43.
- Yu, M., Yang, R., Huang, L., Cao, X., Yang, F., and Liu, D. (2012). "Preparation and characterization of bamboo nanocrystalline cellulose," *BioResources* 7(2), 1802-1812. DOI: 10.15376/biores.7.2.1802-1812
- Zhang, J., Song, H., Zhuang, J., Pang, C., and Liu, S. (2012). "Microfibrillated cellulose from bamboo pulp and its properties," *Biomass Bioenerg.* 39, 78-83. DOI: 10.1016/j.biombioe.2010.06.013

Zhou, L., Yang, Z., Han, X., Jang, S., Dai, J., Yang, B., and Hu, L. (2016). “Thermal conductive, electrical insulating, optically transparent bi-layer nanopaper,” *ACS Appl. Mater. Inter.* 8(42), 28838-28843. DOI: 10.1021/acsami.6b09471

Article submitted: January 25, 2018; Peer review completed: March 17, 2018; Revised version received: April 14, 2018; Accepted: April 21, 2018; Published: April 30, 2018. DOI: 10.15376/biores.13.2.4440-4454